ENVIRONMENTAL RESEARCH
LETTERS

PURPOSE-LED PUBLISHING™
Celebrating the 20th anniversary of Environmental Research Letters

LETTER • **OPEN ACCESS**

Dynamic urban decarbonization pathways revealed in rapidly urbanizing Chinese cities

To cite this article: Tong Chen *et al* 2026 *Environ. Res. Lett.* **21** 204001

View the article online for updates and enhancements.

You may also like

- Eastward displacement of the Pacific–Japan pattern weakens its influence on summertime tropical cyclones affecting China
Yimeng Wang, Jingyun Deng, Peng Hu et al.
- The uncertain impacts of an 1.5 °C overshoot-and-decline scenario on carbon stocks and productivity in terrestrial ecosystems
L E Boeschoten, S J De Hertog, G Recour et al.
- A systematic review of nature-based solutions for climate action in African cities
Nicola Frances Rule, Cameron T McLean, Andrew Emmanuel Okem et al.

This content was downloaded from IP address 131.111.185.132 on 02/11/2026 at 10:02

ENVIRONMENTAL RESEARCH
LETTERS

Check for updates

OPEN ACCESS

RECEIVED
12 February 2026

REVISED
5 October 2026

ACCEPTED FOR PUBLICATION
7 October 2026

PUBLISHED
14 October 2026

Original content from this work may be used under the terms of the Creative Commons Attribution 4.0 licence.

Any further distribution of this work must maintain attribution to the author(s) and the title of the work, journal citation and DOI.

LETTER

Dynamic urban decarbonization pathways revealed in rapidly urbanizing Chinese cities

Tong Chen[1], **Felix Creutzig**[2,3] **and Ramit Debnath**[1,*]

[1] Centre for Human-Inspired AI (CHIA), University of Cambridge, Cambridge, CB2 1PZ, United Kingdom
[2] Bennett Institute for Innovation and Policy Acceleration, University of Sussex Business School, Brighton, United Kingdom
[3] Working Group on Cities, Potsdam Institute for Climate Impact Research (PIK), Potsdam, Germany
[*] Author to whom any correspondence should be addressed.

E-mail: rd545@cam.ac.uk

Keywords: urban decarbonization, city archetypes, carbon emission evolutionary pathways, explainable machine learning

Supplementary material for this article is available online

Abstract

Urban economies and their associated CO_2 emissions depend on a specific urban structure and change dynamically. However, few studies have captured the co-evolution of carbon and broader urban development, or identified the governance-related factors associated with such change across different types of cities. This study addresses this gap by analysing data from 232 Chinese cities between 1999 and 2019. As a key contribution, we investigate urban types as dynamic states by applying *K*-Means++ clustering to pooled city-year observations and identify six archetypes of urban carbon evolution, together with three typical transition pathways. We further apply a low carbon city indicator framework and develop a pooled CatBoost model selected from five candidate algorithms, using SHAP values to interpret archetype-stratified feature contributions to carbon emission predictions. Our identified pathways indicate that carbon control can be compatible with rapid economic development. Cities with similar per capita emissions can nevertheless differ in transition maturity, highlighting distinct capacities and priorities for further decarbonization. SHAP analysis shows that, in earlier industry-led phases, predicted emissions are most strongly associated with industrial-activity and energy-mix indicators; the broader predictor profiles in more mature phases suggest a shift in decarbonization priorities from sector-specific improvements towards systemic action within and across sectors. In particular, Archetype 5 low-carbon leading transition cooling-intensive megacities account for 45% of total emissions in 2019, suggesting that cross-system coordination and the translation of innovation inputs into energy-efficiency improvements and low-carbon infrastructure warrant further assessment as potential mitigation directions. This study develops an integrated framework linking dynamic urban carbon archetypes, development-stage-specific transition pathways, and differentiated policy priorities, providing a diagnostic basis for understanding heterogeneous urban decarbonization transitions.

1. Introduction

As climate change accelerates, cities, which are major centers of energy use and carbon emissions, produce about 62%–72% of global CO_2 [1], making them pivotal to carbon neutrality. Yet cities vary widely in development stages, industrial structures, and energy systems, leading to different emission pathways and decarbonization potentials [2–4]. High-carbon industrial cities, for instance, rely on heavy industry and carbon-intensive energy mixes [5]. As they transition, transport, building efficiency, and innovation capacity gain importance [6–8]. Capturing these shifting drivers is crucial for targeted policies and efficient resource allocation, requiring a move beyond static typologies towards an evolutionary view of where cities are heading.

Research on urban carbon-emission trajectories and their drivers has two main strands. The first is classification. Because urban evolution involves shifts between types, classification underpins the identification of dynamic patterns. Studies commonly group

© 2026 The Author(s). Published by IOP Publishing Ltd

Table 1. Indicators for archetype identification.

Indicator	Mean	Standard deviation	Unit	References
Carbon emissions per capita	14.3	18.0	tCO_2/cap	[23, 26, 40–42]
GDP per capita	5.5	4.0	kUSD[a]	[23, 26, 40–44]
Urbanisation rate	51.0%	16.8%	percentage	[23, 40]
Secondary industry GDP ratio	38.5%	9.2%	percentage	[23, 42, 44]
Natural gas consumption proportion	6.0%	6.9%	percentage	[23, 25, 45]
New energy consumption proportion[b]	6.1%	5.5%	percentage	[23, 25, 45]

[a] The exchange rate for May 23rd 2025 of USD to RMB is approximately 1 USD = 7.2 RMB.
[b] New energy: hydropower, nuclear power, solar power, and wind power.

cities by emission levels and growth trends [9, 10] or by administrative and geographic boundaries [11, 12] to reveal developmental and regional disparities. Others apply tree regression or classify cities by GHG emission drivers at national scales (India [13]; UK [14]) or globally [15]. However, most work is static–based on a single year or short period–so it rarely tracks whether and how cities change categories over time. This limits its policy value, leaving unanswered which cities are likely to transition next and which successful transitions offer transferable lessons.

The second strand examines multidimensional drivers. Using factor decomposition, econometric models, or machine learning, it analyses variables such as energy structure, industrial composition, and spatial layout [12, 16–19]. While this work has expanded understanding of urban carbon systems, indicator choices often reflect data availability rather than governance objectives or policy levers, limiting policy relevance and practical use.

Studies show that city and regional carbon-emission trajectories follow recurring long-term patterns that can be grouped into distinct types [20–22]. Some identify trajectory stages using milestones such as emission peaks and sustained declines [23, 24], while others use decoupling analysis to assess how emissions change relative to economic growth across space and time [25, 26]. Although drivers such as population, industrial structure, energy systems, and other socioeconomic conditions are well recognized [24, 25], most work still focuses on trajectories or turning points. The long-term co-evolution of emissions with multidimensional urban-development states remains underexplored. A dynamic co-evolution analysis is needed to identify intermediate states and multi-stage transition pathways and to align emission-reduction priorities with cities" development stages.

To address these challenges, we treat urban typologies as dynamic and identify year-by-year urban carbon archetypes and their trajectories, rather than using static classifications. Using dynamic clustering, a governance-oriented low-carbon city (LCC) indicator system, and explainable AI (XAI), we analyze emission trajectories and key features using a city-year dataset for 232 Chinese cities (1999–2019). This work advances methods for understanding urban carbon transitions and offers a diagnostic framework applicable to city-level data elsewhere to identify local archetypes and transition patterns.

2. Methods

2.1. Data collection and feature selection

This study compiles panel data for 232 Chinese cities (1999–2019), combining CEADs carbon emissions with 57 LCC planning indicators from statistical yearbooks, municipal records, and official policy documents. Nine control variables capturing demographic, economic, energy, and climatic factors are included. Data were cleaned through imputation, outliers removal, and normalisation. A fully balanced panel is not possible due to regional gaps: eastern coastal cities often have complete 20 year records, while many western or remote cities have shorter series. To maintain coverage of policy-relevant, less developed areas, cities are required to have at least 5 valid years; the average city contributes 13.8 years, with shorter series mostly spanning 2009–2018. While early emissions patterns may be missing for some less developed cities, results for these cities remain relevant for current policy.

A three-step feature selection process improved interpretability and reduced redundancy. Indicators with low variance ($variance < 0.01$) or high multicollinearity ($Pearson's\, R > 0.7$) were removed [27], and only those that were significantly correlated with carbon emissions ($p < 0.05$) were retained. The final LCC planning framework includes 46 indicators across five domains: socioeconomic, energy, transport, environment, and buildings; and innovation and policy (supplementary information A). These indicators are used for archetype-specific SHAP analysis of emission drivers. Archetypes are identified separately using six structural indicators (table 1). Methods for reconstructing missing indicators and the sensitivity analysis are in supplementary information B.

Table 2. Basic characteristics and statistics of 6 archetypes.

Archetype	Archetype 1: High-Carbon Energy-Intensive Industrial Large Cities	Archetype 2: Medium-Carbon Coal-Dependent Growing Small Cities	Archetype 3: Medium-Carbon Middle-Income Regional Core Cities	Archetype 4: Low-Carbon Natural-Gas-Advantaged Cities	Archetype 5: Low-Carbon Leading Transition Cooling-Intensive Megacities	Archetype 6: Low-Carbon New-Energy-Advantaged Coastal Cities
Main characteristics	Energy-based heavy industry; highest per capita emissions; high HDD	Low development baseline, fast growth; coal-dependent energy mix; high carbon lock-in risk	Regional cores; middle to high development; fossil-oriented energy mix	Low emissions; highest natural gas consumption; small and medium cities	Leading transition megacities; highest development stage; highest electrification; strong cooling demand; highest oil consumption	Lowest per-capita emissions; highest new-energy share; incomplete end-use substitution
Spatial characteristics	Northern and central China	Geographically widespread	Central and northern China	Geographically widespread	Southeast coastal China	Southern coastal China
Temporal characteristics	Persistent across 1999 to 2019	Largely before 2014, with some cases persisting thereafter	Mainly after 2010, with some cases persisting thereafter	Mainly after 2005	Mainly after 2012	Mainly 2005 to 2017
Typical city-year	Chongqing (2003–2018); Ordos (2006–2019); Taiyuan (2015–2019)	Shanwei (2000–2019); Zhoushan (2000-2019); Handan (2000–2014)	Zhengzhou (2000–2015); Jinan (1999–2014); Foshan (2001–2006)	Suining (2016–2019); Beihai (2010–2017); Mianyang (2018–2019)	Beijing (2005-2019); Shanghai (2007–2019); Hangzhou (2000–2019)	Zhanjiang (2001–2019); Quanzhou (2005–2014); Jiangmen (2000–2016)

2.2. Identification of carbon emission archetypes

To capture structural heterogeneity across Chinese cities, we clustered six indicators on carbon emissions, economic development, industrial structure, and energy use (table 1), following carbon-emission archetype studies. After Z-score normalisation, we applied K-Means++ (Euclidean distance) to 3201 pooled city-year observations. City-years were clustered independently, allowing city archetypes to change over time. We also tested robustness to indicator selection. The optimal number of clusters ($K = 6$) was chosen using WSS [28], DBI [29], and NMI [30], benchmarked against prior literature and validated with ANOVA and Tukey's HSD tests [31, 32]. See supplementary information C for details.

We computed centroid boundary margins and bootstrap assignment consistency for each city-year to assess boundary uncertainty and stability under changes in the city sample. Boundary cases were flagged when distances to the nearest and second-nearest centroids were similar. The authors jointly reviewed these cases using six clustering indicators and each city's development context to assign final labels, revising 11.9% of labels. Re-identifying pathways with the original labels preserved all four main transition directions, indicating results were not driven by expert adjustments (supplementary information L).

We tracked archetype transitions (1999–2019) to identify typical decarbonisation pathways and grouped cities by shared archetype-change trajectories. Common longitudinal clustering methods (trajectory clustering, group-based trajectory modeling, latent class growth analysis, longitudinal K-means) classify outcome profiles and are not directly suited to sequences of predefined nominal archetypes without extensions [33–36]. Sequence and transition models better fit categorical sequences but require choices about state similarity, duration, alignment, or transition structure [37–39]. Given the clear structure of our data, we used a rule-based method: we ordered each city's annual archetypes; recorded a transition at the first occurrence of a new archetype only if it persisted for at least two consecutive years; collapsed consecutive repeats of confirmed archetypes into one state; then grouped cities with identical simplified sequences and computed pathway frequencies.

Because the main analysis of cities' absolute development states may capture national time trends, we ran robustness checks. We demeaned each clustering indicator by its annual sample median and repeated the analysis with the same six-cluster K-Means++ and pathway procedure, then compared archetype characteristics, city-year assignments, and start-to-end transitions (supplementary information I). To test sensitivity to sample composition, we performed

300 city-level bootstrap resample and reran the clustering to assess the stability of archetypes and pathways (supplementary information K). We also estimated annual archetype persistence and transition probabilities with a Markov model to validate the pathway results (supplementary information M).

2.3. Analysis of indicator predictive contributions

Compared with data-driven, correlation-based, or simple meta-aggregation approaches, LCC indicator systems are grounded in clearer governance logic and policy orientation. Built on understanding low-carbon transition pathways and governance mechanisms, they better capture strategic priorities and multi-level actions, improving interpretability and policy relevance [46, 47]. LCC indicator details are in supplementary information D.

Using the selected indicators, five algorithms (Elastic Net, Random Forest, XGBoost, LightGBM, CatBoost) were compared on 2794 city-year observations from 201 cities (2002–2019), with total city-level carbon emissions as the outcome and 46 LCC indicators as predictors. This sample is smaller than the 3201 observations used for clustering because cases with insufficient indicator coverage were excluded. Most predictors were lagged one year; sunshine duration, wind speed, CDD, and HDD were contemporaneous. CatBoost was chosen as the final pooled model, and predictive performance and SHAP (SHapley Additive exPlanations) results were evaluated by archetype. Model selection and evaluation used nested city-grouped cross-validation. In each of the five outer folds, all observations from the same city were retained in either the training or test subset, with no city appearing in both. Four-fold city-grouped cross-validation within the outer training data was used for preprocessing and hyperparameter selection. Further details are in supplementary information E.

SHAP values [48] were computed for held-out observations in each outer fold of the pooled CatBoost model and grouped by archetype to evaluate the magnitude and direction of each indicator's contribution to carbon-emission predictions. Indicators were ranked by mean absolute SHAP value; the top 15 per archetype were retained. Because the six variables used to define archetypes overlap with the SHAP outcome/explanatory set (carbon emissions is the SHAP outcome; the other five also appear as predictors), results could partly reflect clustering structure: clustering captures between-archetype differences across all city-years, whereas SHAP explains within-archetype variation. To test this, we reran the six-cluster *K*-Means++ and pathway identification excluding per-capita carbon emissions, then refit models without the overlapping predictors and compared performance and SHAP-rank stability (supplementary information J).

3. Results

3.1. Carbon emission evolutionary archetypes characteristics in Chinese cities

We identified six carbon-emission archetypes across 232 Chinese cities (1999–2019), each representing a distinct emission profile, development stage, and spatiotemporal pattern. Table 2 summarizes each archetype's key characteristics and indicator statistics. Figures 1(a) and (b) compare the typological variables, additional descriptive indicators, and spatial distribution. Typological features: emissions, development stage, industrial structure, and energy use, capture structural, long-term drivers of urban carbon profiles. Additional descriptive indicators, while not used for typology, provide complementary context for interpretation. Further details are illustrated in supplementary information F.

Figure 1(b) shows a gradual shift from coal-dependent industrial growth to more diversified, lower-carbon development across Chinese cities. In 2000, medium-carbon coal-dependent growing small cities (Archetype 2) dominated, with only a few Low-Carbon New-Energy-Advantaged Coastal Cities (Archetype 6) along the southeastern coast. By 2010, Archetype 2 was still prevalent in central China, while Archetype 6 expanded southward and Medium-Carbon Middle-Income Regional Core Cities (Archetype 3) and Low-Carbon Natural-Gas-Advantaged Cities (Archetype 4) became more dispersed. By 2019, Low-Carbon Leading Transition Cooling-Intensive Megacities (Archetype 5) clustered along the southeastern coast; Archetype 2 declined markedly, and Archetype 3 remained relatively stable.

Archetype 1 High-Carbon Energy-Intensive Industrial Large Cities are northern and central China cities with heavy, energy-intensive industry and high-temperature processes. They have the highest per capita emissions (58.5 tCO_2/cap). The energy mix is improving as coal and oil shares fall; coal still dominates but declines, while natural gas and electrification rise. They are heating-dominated with high HDD.

Archetype 2 Medium-Carbon Coal-Dependent Growing Small Cities are rapidly growing, low-baseline third- and fourth-tier cities and early-stage large cities. They have the second-highest per capita emissions (14.9 tCO_2/cap). Their pathway is the most coal-dependent, with the highest coal share and the lowest natural gas, new energy, and electrification rates, indicating high carbon lock-in risk.

Archetype 3 medium-carbon, middle-income regional core cities, provincial capitals and regional hubs that became more common after 2010, are at a mid-to-high development stage, with secondary and tertiary industry shares both ranking second. However, their transition lags: the energy mix remains fossil-based, and the shares of natural gas and new energy consumption both rank fifth. Per

capita emissions rank third, and heating demand is relatively high, with HDD ranking second.

Archetype 4 Low-Carbon Natural-Gas-Advantaged Cities are mostly small and medium-sized cities with relatively low emissions and the highest natural-gas share (17.7%). Their per-capita emissions rank fifth, but deeper transition is limited: new energy ranks fourth and electrification fifth.

Archetype 5 Low-Carbon Leading Transition Cooling-Intensive Megacities are national front runners along the southeast coast. Despite slowing growth, they show the strongest end-use transition, with the highest electrification and relatively high natural gas and new energy shares. They also have the highest oil share, likely reflecting high road-transport activity and vehicle stocks. Cooling demand is highest (highest CDD, second-lowest HDD).

Archetype 6 Low-Carbon New-Energy-Advantaged Coastal Cities are small and medium coastal cities, often on the edge of southern urban agglomerations. They have the lowest per-capita emissions (8.7 tCO_2/cap) and the highest new-energy share (11.9%). End-use substitution is incomplete, with the highest LPG share and electrification ranking fourth. Oil ranks second, and cooling demand is strong (CDD second, HDD lowest).

Overall, the six archetypes differ systematically in development, industrial structure, and decarbonisation conditions. Higher-emission cities (Archetypes 1–3) are shaped by heavy industry and limited clean energy, while lower-carbon cities (Archetypes 4–6) follow varied pathways via gas substitution, high-tech leadership, or renewable-resource alignment. City lists are in supplementary data 1.

3.2. Temporal evolution of archetypes and three main transition pathways

Figure 2(a) shows how cities' archetypes changed over two decades. Archetype 2 declined over time, while Archetypes 3 and 5 grew to become most prevalent. We identified three main transition pathways based on cities" archetype membership over time (figure 2(d)).

First, many Medium-Carbon Coal-Dependent Growing Small Cities (Archetype 2) transitioned to Archetype 3 Medium-Carbon Middle-Income Regional Core Cities (19.8%, $n = 46$) or Archetype 4 Low-Carbon Natural-Gas-Advantaged Cities (10.8%, $n = 25$), indicating two main expansion-stage pathways. Along the Archetype 2-to-3 pathway, per-capita carbon emissions fell 40.9%, while GDP per capita rose 100.7% and urbanization increased by 14.1 percentage points. The coal share declined by 8.7 percentage points, while natural-gas and new-energy shares rose by 2.2 and 2.6 percentage points (supplementary information F), indicating industrial consolidation with partial energy decarbonisation (e.g. Zhangjiakou, Dezhou). In contrast, the Archetype 2-to-4 pathway featured a larger coal-share drop (−13.0 percentage points) and a sharp rise in natural-gas share (+8.9 percentage points). Despite continued GDP and urbanisation growth, per-capita emissions fell 34.5%, reflecting faster coal phase-down driven by increased natural-gas use (e.g. Yan'an, Chuzhou).

Second, 12 Medium-Carbon Middle-Income Regional Core Cities (Archetype 3) transitioned to Low-Carbon Leading Transition Cooling-Intensive Megacities (Archetype 5) (5.2%, $n = 12$). GDP per capita rose 148.1%. In all 12 cities, per-capita science and technology and education spending increased; city-weighted pathway averages rose 577.7% and 256.2%. Green patent authorizations per 10 000 people increased 1312.1%. Coal's share fell 11.5 percentage points, new energy rose 3.3 points, and electrification rose 5.8 points, while per-capita carbon emissions were broadly stable. Overall, the shift to Archetype 5 reflects cleaner, more innovation-intensive development alongside a substantial industrial base; several cities were also covered by low-carbon pilot policies (e.g. Beijing, Shanghai, Tianjin, Nanjing).

Third, some Low-Carbon New-Energy-Advantaged Coastal Cities (Archetype 6) shifted to Archetype 5 after 2010/2015 (6.0%, $n = 14$). Per-capita emissions fell 34.0%, while GDP per capita rose 289.4% and urbanization increased by 17.0 percentage points. Electrification and the new-energy share rose by 24.9 and 6.4 percentage points, with the new-energy share averaging 17.0% in the final stage. Overall, this pathway reflects stronger new-energy advantages, higher end-use electrification, growing urban/industrial activity, and a sharper drop in per-capita emissions (e.g. Quanzhou).

We find 8.2% of cities ($n = 19$) moved from Archetype 2 to Archetype 5 (figure 2(d)), showing a pathway of economic growth with lower per-capita emissions. Of these, 16 used Archetype 3 as an intermediate and 4 used Archetype 6; Three cities passed through both intermediate archetypes and were therefore counted in both categories. These counts represent unique cities rather than city-year transitions, reflecting multiple routes to Archetype 5. Across these cities, GDP per capita increased by 280.4% and urbanization rose by 23.7 percentage points, while carbon emissions per capita decreased by 20.1%. The coal consumption share declined by 5.9 percentage points, the new-energy consumption share increased by 5.7 percentage points, and per-capita scientific and technological expenditure and per-capita education expenditure increased in every city. The different intermediate states reveal two complementary profiles: Archetype 3 primarily provides stronger industrial, urban, and innovation

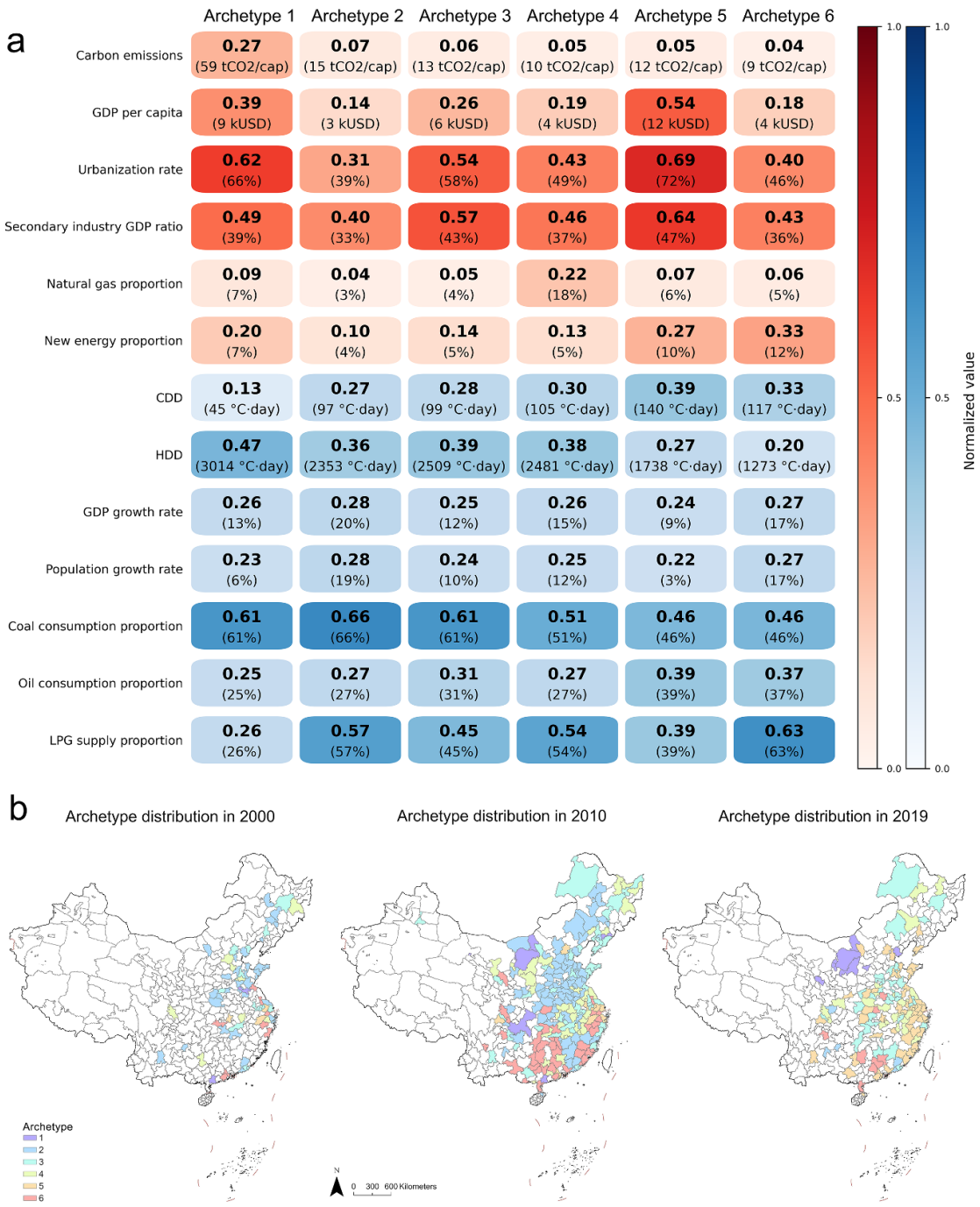


Figure 1. (a), Heatmap of properties of cities used for typological (red) and additional descriptive characterization (blue), with values normalized to facilitate inter-group comparison. (b), Spatial distribution of archetypes in 2000, 2010, and 2019.

capacities, whereas Archetype 6 provides a stronger new-energy foundation. Their eventual convergence towards Archetype 5 shows that cities with different intermediate advantages can reach the same, more mature transition state. By contrast, 4.7% of cities stayed in Archetype 2 and 9.1% stayed in Archetype 4 over two decades, suggesting lock-in to coal dependence or a natural-gas transition. City lists are in supplementary data 2, with further details in supplementary information H.

After removing annual medians, the Archetype 3 → 5 transition remained, and the Archetype 2 → 4 pathway persisted at a lower frequency. Archetype 2 → 3 and 6 → 5 were more affected, suggesting they partly reflected national development trends. Despite differing robustness, the adjusted analysis preserved a similar six-group structure and key transition directions, underscoring city-specific structural change in archetype differentiation and transition (supplementary information I).

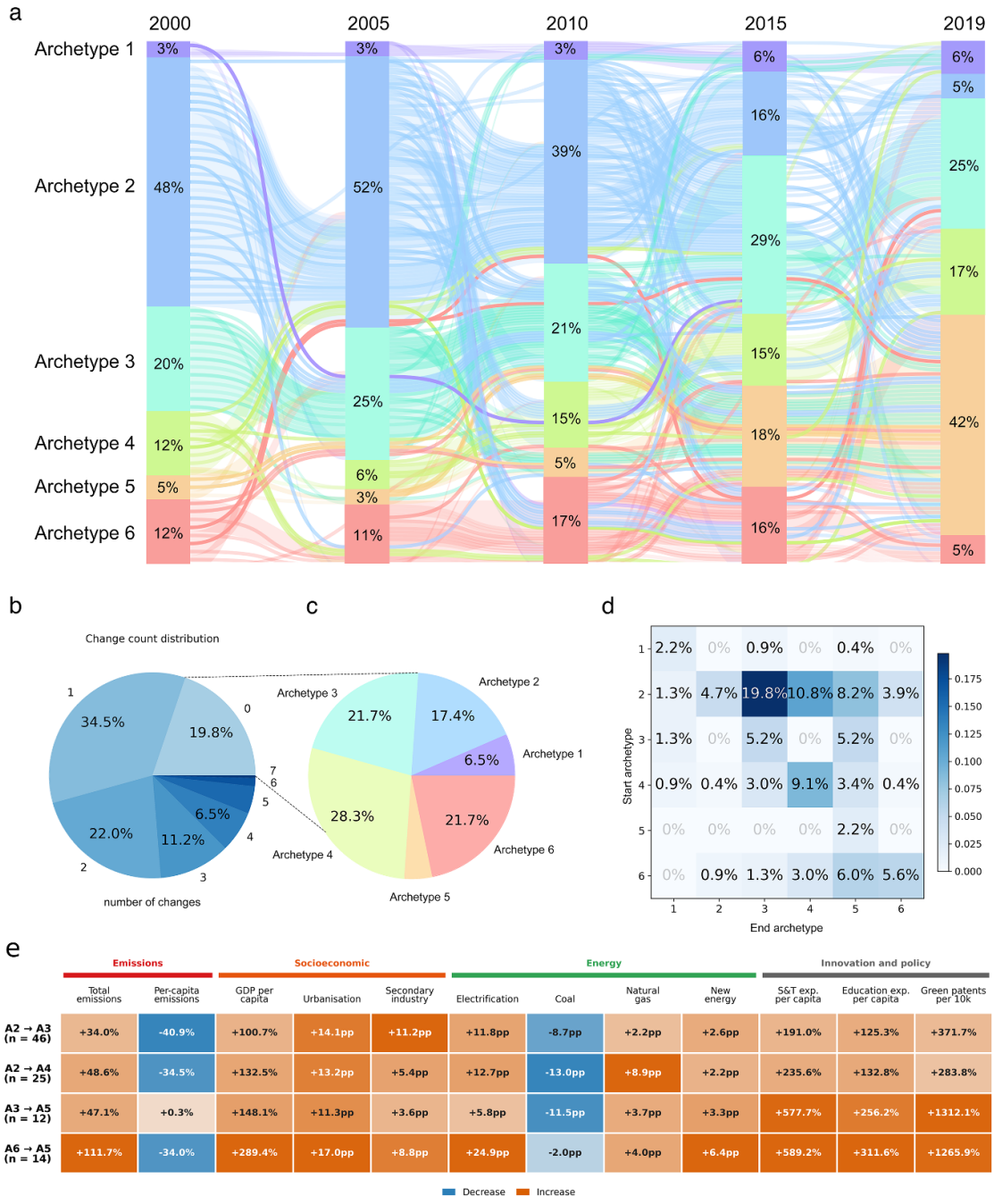


Figure 2. (a), Temporal transitions among archetypes. Column heights indicate the share of cities in each archetype at five benchmark years. Curved ribbons trace city-level trajectories; line color is fixed by the origin archetype. (b), Distribution of transition counts per city. (c), Composition of cities with no archetype change. (d), Origin–destination matrix of archetypes derived from simplified paths. Values denote the fraction of all cities whose start archetype (first archetype in the simplified path) and end archetype (last archetype in the simplified path) correspond to the row and column, respectively. (e), Changes in selected indicators along the four major transition pathways. Values compare city-weighted means during each city's initial and final continuous archetype periods. The symbol % denotes relative change in level variables, whereas pp denotes the arithmetic percentage-point change in rates and shares. GDP pc denotes GDP per capita; S&T exp. pc denotes scientific and technological expenditure per capita; Edu. exp. pc denotes education expenditure per capita; and Green patents per 10k denotes green patent authorisations per 10 000 people.

Bootstrap results showed mean ARI = 0.604 and mean assignment agreement = 80.0%. All four pathway proportions lay within their 95% bootstrap intervals, indicating generally stable transition directions (supplementary information K). A Markov-model robustness test also supported these principal directions (supplementary information M).

3.3. Predictive performance and LCC indicator associations across six archetypes

This study uses the LCC indicator system [46, 47] to identify indicators most associated with carbon-emission predictions across archetypes. Table 3 reports sample composition and archetype-stratified performance under five-fold city-grouped

out-of-fold evaluation. Performance is comparable to recent studies using socioeconomic, energy, built-environment, and remote-sensing predictors, which reported $R^2 \approx 0.77$–0.88 under city-grouped cross-validation or hold-out evaluation [49–51]. Archetype 1 showed lower out-of-fold stability due to limited sample size. Across all six archetypes, coal consumption, natural gas consumption, new energy consumption, man-made coal gas supply, and HDD consistently ranked among the top 15 indicators (figure 3).

For Archetype 1 (High-Carbon, Energy-Intensive Industrial Large Cities), industrial enterprise count had the highest mean absolute SHAP value and was positively linked to emissions. Coal consumption proportion and HDD ranked 2nd and 3rd and also increased emissions. Man-made coal gas supply, road area, vehicle ownership, and industrial electricity consumption showed similar positive effects. In contrast, new energy and natural gas consumption proportions (12th and 13th) were associated with lower emissions, underscoring the need to shift the energy mix while managing industrial growth.

For Archetype 2 (Medium-Carbon, Coal-Dependent Growing Small Cities), coal consumption proportion was the top SHAP indicator and increased emissions, followed by HDD and man-made coal gas supply. New energy and natural gas consumption proportions ranked 5th and 6th and reduced emissions. Road area, construction land, population, GDP, roads-and-bridges investment, and new fixed assets were generally linked to higher emissions, reflecting carbon pressures from rapid urban expansion.

In Archetype 3 (Medium-Carbon Middle-Income Regional Core Cities), man-made coal gas supply had the highest mean absolute SHAP value and was positively linked to emissions, followed by population, coal consumption proportion, and GDP. Natural gas and new energy consumption proportions (5th and 7th) were linked to lower emissions. HDD, vehicle ownership, road area, and annual new fixed assets were linked to higher emissions, implying that cleaner energy substitution must accompany ongoing economic, transport, and infrastructure growth (see figure 4).

In Archetype 4 (Low-Carbon Natural-Gas-Advantaged Cities), natural gas consumption proportion had the highest SHAP value and was linked to lower emissions, while coal consumption proportion and man-made coal gas supply (2nd and 3rd) were linked to higher emissions. Population, road area, HDD, industrial electricity intensity, and the number of industrial enterprises were also positively linked to emissions, whereas new energy consumption proportion reduced emissions. This suggests reinforcing the natural-gas advantage through further substitution and managing demand from expansion.

In Archetype 5 (Low-Carbon Leading Transition Cooling-Intensive Megacities), coal consumption proportion remained the strongest positive driver. Green patent authorizations and education expenditure also ranked highly, reflecting their association with these cities" large economic scale and transition activity. New energy consumption proportion (3rd) was linked to lower emissions; total electricity consumption and natural gas consumption proportion were also negatively associated. Road area, GDP, tertiary-industry activity, and industrial electricity intensity were positively linked to emissions, indicating more broadly distributed drivers across urban systems (see figure 4).

In Archetype 6 Low-Carbon New-Energy-Advantaged Coastal Cities, man-made coal gas supply had the highest mean absolute SHAP value and was positively associated with emissions. New energy consumption proportion ranked second and was linked to lower emissions; coal consumption proportion and HDD ranked third and fourth and increased emissions. Natural gas, oil, LPG supply, and total electricity consumption were linked to lower emissions, while population, GDP, and industrial electricity intensity increased emissions. This underscores the need to preserve the new-energy advantage while reducing reliance on carbon-intensive industrial and gas-supply systems. See supplementary information E.

Sensitivity analysis indicated that excluding carbon emissions per capita still produced classifications broadly consistent with the baseline (ARI $= 0.775$) and preserved key transitions (A2 $\rightarrow$ A3, A2 $\rightarrow$ A4, A6 $\rightarrow$ A5). Removing predictors overlapping with clustering indicators led to only a small performance drop ($\Delta R^2 = -0.025$), while archetype-specific SHAP rankings stayed stable, retaining 12–13 of the top 15 predictors (supplementary information J).

4. Discussion

This study identifies dynamic evolutionary pathways of urban carbon-emission archetypes and the factors linked to more sustainable transitions. Using data for 232 Chinese cities (1999–2019), we identify six archetypes and three representative trajectories and apply the low carbon cities (LCCs) indicator framework and XAI to highlight the indicators most strongly associated with predicted outcomes.

A key contribution is the six-archetype typology, showing that decarbonisation trajectories depend more on transition maturity than on emission levels alone. Existing classifications typically group cities by development stage and production–energy systems, with density, urban form, climate, and transport explaining additional variation [13–15, 44]. However, because they usually rely on cross-sectional emissions and structural features, they rarely distinguish transition maturity among cities

Table 3. Sample sizes and out-of-fold predictive performance of the pooled CatBoost model.

Scope	Observations	R^2	RMSE	MAE
Overall	2794	0.824	17.67	10.46
Archetype 1	133	0.650	53.79	35.15
Archetype 2	888	0.846	10.60	7.56
Archetype 3	749	0.817	15.79	11.02
Archetype 4	301	0.725	14.59	9.54
Archetype 5	363	0.863	18.75	14.58
Archetype 6	360	0.821	5.07	3.92

Observations refer to city-year observations. All rows evaluate the same pooled CatBoost model using predictions for cities excluded from the corresponding outer-fold training data. RMSE and MAE are expressed in $MtCO_2$.

with similar emissions or track long-term change within a consistent framework. Our results show that similar emission levels can reflect different transition foundations and capacities. For Archetypes 4–6, comparable low per-capita emissions imply different next steps, from moving beyond gas substitution to extending end-use electrification and coordinating changes across urban systems. Pooling city-year observations also yields temporally comparable archetypes that enable tracking long-term evolutionary pathways.

Another contribution is identifying dynamic pathways, as illustrated in figure 4. Unlike single-year or period-average classifications, this approach shows both a city's archetype at a given time and the roles of intermediate states. The three pathways illustrate how rapidly urbanizing Chinese cities balance emissions control and economic growth.

Pathway 1 is a shift from Archetype 2 to 3 or 4, likely reflecting natural-gas infrastructure expansion, coal-to-gas programs, industrial upgrading, and regional coordination [52–55]. Research on Zhangjiakou also suggests that combining renewable energy substitution with industrial restructuring can cut energy use and greenhouse-gas emissions [56].

Pathway 2 describes the shift from Archetype 3 to Archetype 5, linked to low-carbon pilot programs and the integration of finance and technology into urban economies [57, 58]. Beijing, Shanghai, and Tianjin are examples of low-carbon pilot cities on this pathway. Quasi-experimental evidence shows the policy reduced emissions more strongly in municipalities and boosted low-carbon innovation by improving the innovation environment and resource allocation [59, 60]. Pathway 3 links Archetype 6 and Archetype 5, marked by a new-energy advantage, growing end-use electrification, and lower emissions. Studies also find that renewable expansion must be coordinated with transmission, storage, demand response, and load flexibility [61, 62].

Additionally, 8.2% of cities fully transitioned from Archetype 2, via Archetype 3, 4, or 6, to Archetype 5 (figure 4). These sequences reflect historical patterns, not required steps for future decarbonization. Future Archetype 2 cities may not need a natural-gas phase: dynamic least-cost analysis suggests that premature investment in long-lived gas infrastructure can delay photovoltaics and electrification in some regions, so pathways may shift with technology costs, infrastructure, and policy conditions [63]. A direct coal-to-renewable-and-grid transition is therefore a policy option, subject to local resource and grid-capacity assessment. These pathways are especially relevant for the 11 cities still in Archetype 2 and the 21 that remained in Archetype 4 over the two-decade study. The study links static city types into an ordered transition process: cities can build industrial and innovation capacity or use new-energy advantages to reach intermediate stages before converging on a low-carbon leading state.

These pathways and archetype-specific SHAP results suggest that decarbonisation policy should begin with sectoral shifts, especially in industry, and become more systemic, requiring cross-sector measures and stronger linkages. In 2019, Archetype 5 (Low-Carbon Leading Transition Cooling-Intensive Megacities) produced 45% of total city emissions (3.1 Gt CO_2), far more than any other archetype, largely because it includes many large cities. SHAP results show predictive contributions for this archetype across the widest range of urban systems, suggesting–together with the literature–that clean electrification is a promising option. High research, innovation, and education inputs currently appear to reflect urban scale more than mitigation benefits, implying a need to better translate innovation into energy-efficiency and low-carbon infrastructure gains [60, 64].

Archetypes 1 and 3 form the next tier, accounting for 24% (1.6 Gt CO_2) and 19% (1.3 Gt CO_2) of archetype emissions in 2019. In both, coal and manufactured gas contribute positively to predicted emissions, while new energy contributes negatively, underscoring clean electrification as a key

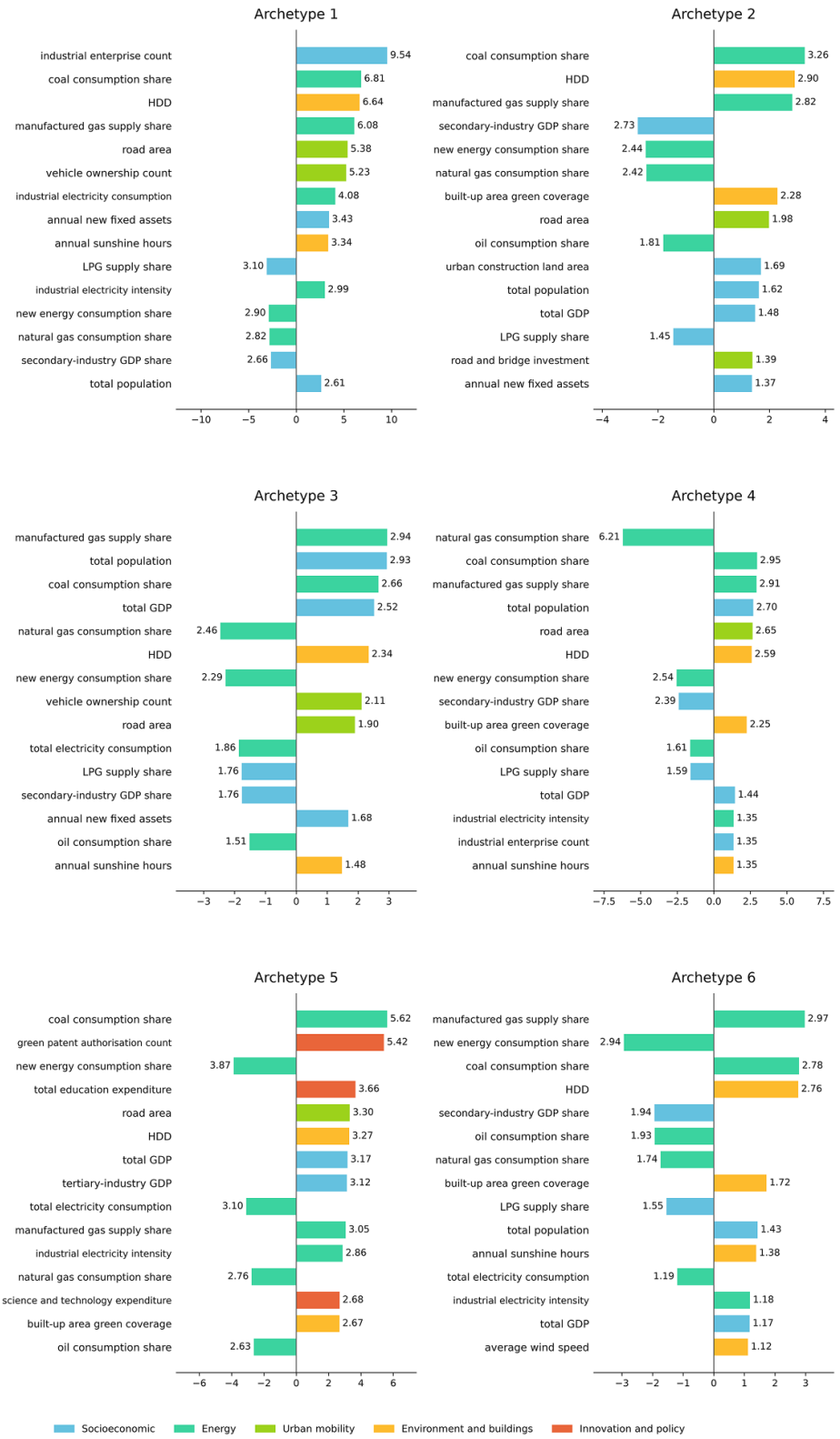


Figure 3. Archetype-stratified out-of-fold SHAP results from the pooled CatBoost model. The top 15 indicators within each archetype are ranked by their mean absolute SHAP values. Indicators are selected based on the Low-Carbon City indicator system [46, 47].

option. Archetype 1 may prioritize electrifying high-temperature industrial processes alongside power-sector decarbonisation and process needs [65], but its limited observations warrant caution in interpreting indicator rankings. Archetype 3 may phase out coal-fired heating and industrial boilers by shifting to new energy and using low-carbon pilot policies to support a transition towards Archetype 5 [59, 66].

Archetypes 4, 6, and 2 contribute smaller shares–8% (0.57 Gt CO_2), 3% (0.18 Gt CO_2), and 2%

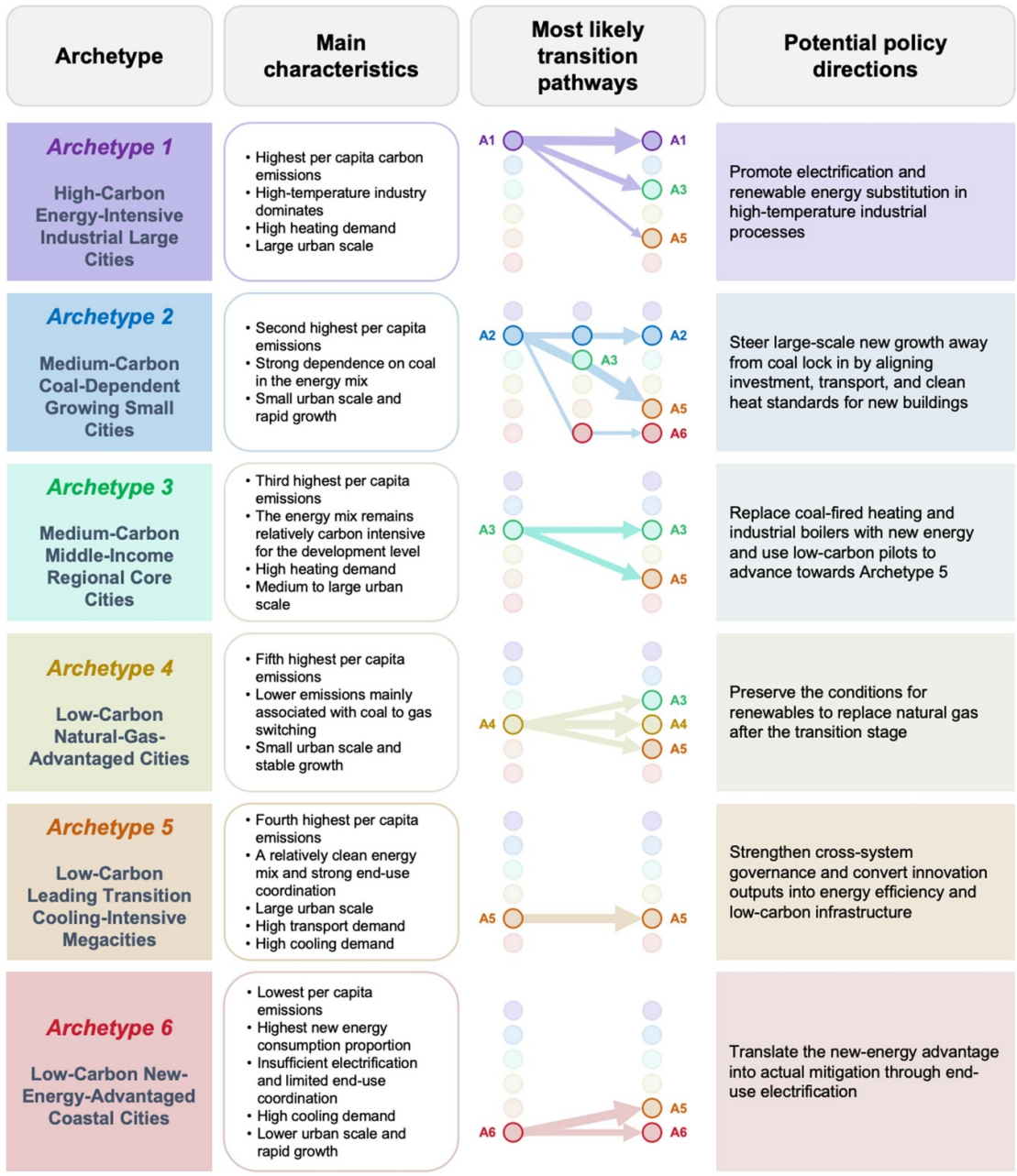


Figure 4. Potential policy directions by archetype. For the most likely transition pathways, thicker lines indicate a greater likelihood of occurrence, which is based on the statistics from figure 2(d).

(0.15 Gt CO_2), respectively. Across them, manufactured gas, coal, and urban-expansion variables are key predictors. Along with pathway evidence, this points to avoiding new high-carbon lock-in during rapid construction. Archetype-specific priorities include enabling renewables to replace natural gas after the transition in Archetype 4, turning the new-energy advantage into end-use electrification in Archetype 6, and setting higher energy and carbon standards before new industries and infrastructure take hold in Archetype 2 (figure 4).

These findings suggest three policy implications for Chinese cities. First, frameworks should move beyond geographic categories to archetypes reflecting emission trajectories and development stages, enabling experience-sharing and policy diffusion among peer cities. Second, fiscal allocation should include archetype-specific incentives targeting priority areas [67]. Third, low-carbon pilot policies should be chosen and implemented in phases aligned with identified transition pathways; the '2–3/4/6–5' trajectory highlights the value of pilot-based approaches. The framework could also serve as a comparative and diagnostic tool in other countries with similar longitudinal city-level data, with indicators adapted to local resources, development patterns, and institutions. By combining pooled city-year clustering, longitudinal tracking of archetype membership, and pooled predictive modeling with archetype-stratified interpretation, it offers a consistent method

to identify locally grounded urban types and transition patterns.

This study has limitations. City coverage is incomplete, especially in western China, possibly under-representing less-developed regions and their transition patterns. The analysis omits hard-to-measure factors (behaviour, enforcement, international influences). Associating archetypes with policy contexts does not pinpoint the drivers of turning points, and observational machine-learning models cannot infer causality. Future work should broaden data coverage, add variables via surveys, proxies, or text analysis, and use event-study and causal-inference methods.

Nonetheless, this study advances urban decarbonisation research by converting urban types into temporally comparable states and linking them through observable transition sequences. Decarbonization trajectories depend on a city's transition maturity, not just its emission level. Although Archetypes 4–6 have similar per capita emissions, they differ in capacity and options for further decarbonisation. Results suggest transitions begin with sectoral shifts, especially in industry, and become more systemic as cities mature. For Archetype 5, further progress requires cross-sector measures and stronger sectoral linkages. The framework helps diagnose the transition stage, learn from comparable cities, and identify locally appropriate pathways.

Future work should expand geographic coverage and add behavioural, institutional, and international indicators for a fuller view of urban transitions. Event studies and causal-inference approaches could test mechanisms behind the observed associations.

Acknowledgments

R D acknowledges the support of the Minderoo Foundation and the climaTRACES Lab (now the Center for Space, Earth and Energy (CSEE)) at CRASSH, University of Cambridge. T Chen and R D acknowledge the support of the UKRI ESRC CDT (Grant number: ES/Y001788/1) at the University of Cambridge.

Data availability statement

All data that support the findings of this study are included within the article (and any supplementary files).

Supplementary information 1 available at https://doi.org/10.1088/1748-9326/aeb14a/data1.

Conflict of interests

F C is a guest editor for ERL's special issue on 'Cities and Climate Change: Systematic Reviews and Typologies'.

Author contributions

Tong Chen 0000-0002-8242-2412
Conceptualization (equal), Data curation (lead), Formal analysis (lead), Methodology (lead), Visualization (lead), Writing – review & editing (equal)

Felix Creutzig 0000-0002-5710-3348
Conceptualization (equal), Supervision (equal), Validation (equal), Writing – original draft (equal), Writing – review & editing (equal)

Ramit Debnath 0000-0003-0727-5683
Conceptualization (equal), Funding acquisition (equal), Methodology (equal), Project administration (equal), Resources (equal), Supervision (equal), Validation (equal), Writing – original draft (equal), Writing – review & editing (equal)

References

[1] IPCC 2022 *Climate Change 2022: Mitigation of Climate Change. Contribution of Working Group III to the Sixth Assessment Report of the Intergovernmental Panel on Climate Change* (Cambridge University Press) section B.2.3, Urban-related emission share pp 3–35

[2] Lwasa S *et al* 2022 *Climate Change 2022: Mitigation of Climate Change. Contribution of Working Group III to the Sixth Assessment Report of the Intergovernmental Panel on Climate Change* ed P R Shukla *et al* (Cambridge University Press)

[3] Wang R, Zheng X, Wang H and Shan Y 2019 Emission drivers of cities at different industrialization phases in china *J. Environ. Manage.* **250** 109494

[4] Ma L, Cheng T, Xiang L, Wang C, Wei L, Wang J, Dang C, Fu W and Wu H 2025 Chinese cities show disparity trends in carbon efficiency: a hybrid approach combining explainable machine learning and econometrics *Sustain. Cities Soc.* **127** 106455

[5] Yang Y, Yu S and Sun Y F 2024 Restructuring effects of industrial and energy structures on sectoral CO_2 emission peak trajectories in china *iScience* **27** 110541

[6] Shan H and Shao S 2024 Impact of green innovation on carbon reduction in china *Sci. Rep.* **14** 14032

[7] Cabeza L F *et al* 2022 *Climate Change 2022: Mitigation of Climate Change. Contribution of Working Group III to the Sixth Assessment Report of the Intergovernmental Panel on Climate Change* ed P R Shukla *et al* (Cambridge University Press)

[8] Sims R *et al* 2022 *Climate Change 2022: Mitigation of Climate Change. Contribution of Working Group III to the Sixth Assessment Report of the Intergovernmental Panel on Climate Change* ed P R Shukla *et al* (Cambridge University Press)

[9] Duan C, Zhu W, Wang S and Chen B 2022 Drivers of global carbon emissions 1990–2014 *J. Clean. Prod.* **371** 133371

[10] Ozturk F, Keles M and Evrendilek F 2016 Quantifying rates and drivers of change in long-term sector- and country-specific trends of carbon dioxide-equivalent greenhouse gas emissions *Renew. Sustain. Energy Rev.* **65** 823–31

[11] Xu P, Zhou G, Zhao Q, Lu Y and Chen J 2024 Spatial-temporal dynamics and influencing factors of city level carbon emission of mainland china *Ecol. Indic.* **167** 112672

[12] Cai A, Wang L, Zhang Y, Wu H, Zhang H, Guo R and Wu J 2025 Uncovering the multiple socio-economic driving

factors of carbon emissions in nine urban agglomerations of china based on machine learning *Energy* **319** 134859
[13] Ahmad S and Creutzig F 2019 Spatially contextualized analysis of energy use for commuting in india *Environ. Res. Lett.* **14** 045007
[14] Baiocchi G, Creutzig F, Minx J and Pichler P-P 2015 A spatial typology of human settlements and their co2 emissions in England *Glob. Environ. Change* **34** 13–21
[15] Creutzig F, Baiocchi G, Bierkandt R, Pichler P-P and Seto K C 2015 Global typology of urban energy use and potentials for an urbanization mitigation wedge *Proc. Natl Acad. Sci.* **112** 6283–8
[16] Ma X, Wang C, Dong B, Gu G, Chen R, Li Y, Zou H, Zhang W and Li Q 2019 Carbon emissions from energy consumption in china: its measurement and driving factors *Sci. Total Environ.* **648** 1411–20
[17] Fan Y, Liu L-C, Wu G and Wei Y-M 2006 Analyzing impact factors of co2 emissions using the stirpat model *Environ. Impact Assess. Rev.* **26** 377–95
[18] Khan K and Su C-W 2021 Urbanization and carbon emissions: a panel threshold analysis *Environ. Sci. Pollut. Res.* **28** 26073–81
[19] Gao Z, Zhou P and Wen W 2025 What drives urban low-carbon transition? findings from china *Environ. Impact Assess. Rev.* **110** 107679
[20] Luqman M, Rayner P J and Gurney K R 2023 On the impact of urbanisation on CO_2 emissions *npj Urban Sustain.* **3** 6
[21] Yang X, Jin K, Duan Z, Gao Y, Sun Y and Gao C 2024 Spatial-temporal differentiation and influencing factors of carbon emission trajectory in chinese cities - a case study of 247 prefecture-level cities *Sci. Total Environ.* **928** 172325
[22] Trejo-Jerónimo Y, López-Flores F J, Ramírez-Márquez C, Lira-Barragán L F and Ponce-Ortega J M 2025 Greenhouse gas emission clustering: advancing net-zero goals through data-driven analysis *Ind. Eng. Chem. Res.* **64** 7466–88
[23] Lin H, Zhou Z, Chen S and Jiang P 2023 Clustering and assessing carbon peak statuses of typical cities in underdeveloped western china *Appl. Energy* **329** 120299
[24] Shan Y, Guan Y, Hang Y, Zheng H, Li Y, Guan D, Li J, Zhou Y, Li L and Hubacek K 2022 City-level emission peak and drivers in china *Sci. Bull.* **67** 1910–20
[25] Shen L, Wu Y, Shuai C, Lu W, Chau K and Chen X 2018 Analysis on the evolution of low carbon city from process characteristic perspective *J. Clean. Prod.* **187** 348–60
[26] Li W, Ji Z and Dong F 2022 Spatio-temporal analysis of decoupling and spatial clustering decomposition of CO_2 emissions in 335 chinese cities *Sustain. Cities Soc.* **86** 104156
[27] Dormann C F *et al* 2013 Collinearity: a review of methods to deal with it and a simulation study evaluating their performance *Ecography* **36** 27–46
[28] Syakur M A, Khotimah B K, Rochman E M S and Satoto B D 2018 Integration k-means clustering method and elbow method for identification of the best customer profile cluster *IOP Conf. Ser.: Mater. Sci. Eng.* **336** 012017
[29] Mughnyanti M, Efendi S and Zarlis M 2020 Analysis of determining centroid clustering x-means algorithm with davies-bouldin index evaluation *IOP Conf. Ser.: Mater. Sci. Eng.* **725** 012128
[30] McDaid A F, Greene D and Hurley N 2013 Normalized mutual information to evaluate overlapping community finding algorithms (arXiv:1110.2515 [physics.soc-ph])
[31] Sthle L and Wold S 1989 Analysis of variance (anova) *Chemometr. Intell. Lab. Syst.* **6** 259–72
[32] Tukey J W 1949 Comparing individual means in the analysis of variance *Biometrics* **5** 99–114
[33] Montero P and Vilar J A 2014 TSclust: an R package for time series clustering *J. Stat. Softw.* **62** 1–43
[34] Nagin D S 1999 Analyzing developmental trajectories: a semiparametric, group-based approach *Psychol. Methods* **4** 139–57
[35] Jung T and Wickrama K A S 2008 An introduction to latent class growth analysis and growth mixture modeling *Soc. Personal. Psychol. Compass* **2** 302–17
[36] Genolini C and Falissard B 2010 KmL: K-means for longitudinal data *Comput. Stat.* **25** 317–28
[37] Gabadinho A, Ritschard G, Müller N S and Studer M 2011 Analyzing and visualizing state sequences in R with TraMineR *J. Stat. Softw.* **40** 1–37
[38] Bartolucci F, Pandolfi S and Pennoni F 2017 LMest: an R package for latent markov models for longitudinal categorical data *J. Stat. Softw.* **81** 1–38
[39] Helske S and Helske J 2019 Mixture hidden markov models for sequence data: the seqHMM package in R *J. Stat. Softw.* **88** 1–32
[40] Feng X, Wang S, Wu N, Li Y and Yang J 2025 Urban low-carbon governance zoning coupled with urban attributes and spatial networks: theoretical framework and practical path *J. Environ. Manage.* **373** 123865
[41] Wei W and Bofeng C 2021 Analysis of carbon emission types and carbon management pathways in chinese cities *Urban Manag. Technol.* **22** 18–21
[42] Li S, Sum Z, Wen R, Yang H, Li J, Chen T, Zheng Y and Zhu N 2018 Spatiotemporal patterns and the influence mechanism of urban landscape pattern on carbon emission performance: evidence from Chinese cities *Resour. Dev. Mark.* **118** 106042
[43] Cheng S, Fan W, Zhang J, Wang N, Meng F and Liu G 2021 Multi-sectoral determinants of carbon emission inequality in chinese clustering cities *Energy* **214** 118944
[44] Shan Y *et al* 2018 City-level climate change mitigation in china *Sci. Adv.* **4** eaaq0390
[45] Jiang J, Ye B, Xie D and Tang J 2017 Provincial-level carbon emission drivers and emission reduction strategies in china: combining multi-layer lmdi decomposition with hierarchical clustering *J. Clean. Prod.* **169** 178–90
[46] Tan S, Yang J, Yan J, Lee C, Hashim H and Chen B 2017 A holistic low carbon city indicator framework for sustainable development *Appl. Energy* **185** 1919–30
[47] Du X, Shen L, Ren Y and Meng C 2022 A dimensional perspective-based analysis on the practice of low carbon city in china *Environ. Impact Assess. Rev.* **95** 106768
[48] Lundberg S M and Lee S-I 2017 A unified approach to interpreting model predictions *Advances in Neural Information Processing Systems* vol 30, ed I Guyon, U V Luxburg, S Bengio, H Wallach, R Fergus, S Vishwanathan and R Garnett (Curran Associates, Inc)
[49] Hsu A, Wang X, Tan J, Toh W and Goyal N 2022 Predicting european cities' climate mitigation performance using machine learning *Nat. Commun.* **13** 7487
[50] Chen X and Ba Y 2026 City-level carbon emissions data in Southeast Asia from 2000 to 2020 *Sci. Data* **13** 964
[51] Yu Y, Wang X, Manya D and Hsu A 2026 Machine learning estimates for G20 subnational urban GHG emissions from 2000–2020 *Sci. Data* **13** 487
[52] (JICA) J I C A 2006 Final report on the basic survey on the revitalization of the northeast region of the people's republic of china (part II) *Technical Report* (National Development and Reform Commission) Commissioned by the Department of Regional Economy, National Development and Reform Commission, China (available at: https://openjicareport.jica.go.jp/pdf/11826237.pdf)
[53] For the Coordinated Development of the Beijing-Tianjin-Hebei Region, L G 2015 Outline of coordinated development of the beijing-tianjin-hebei region Chinese. Approved at the Political Bureau Meeting of the CPC Central Committee. Initially reviewed on February 10, 2015, by the Central Leading Group for Financial and Economic Affairs. Officially approved on 30 April 2015. The Outline identifies coordinated development of Beijing-Tianjin-Hebei as a major national strategy, with a focus on relieving Beijing of non-capital functions and promoting breakthroughs in transportation integration, environmental protection, and industrial upgrading
[54] For Promoting the Development of the Yangtze River Economic Belt, L G 2016 Outline of the development plan

for the Yangtze River economic belt Chinese. Approved at the Political Bureau Meeting of the CPC Central Committee on 25 March 2016. The Outline presents a strategic plan for the Yangtze River Economic Belt, covering ecological protection, integrated transportation systems, industrial upgrading, new urbanization, and regional coordination. It defines the 'one axis, two wings, three poles, and multiple points' spatial strategy, and serves as a guiding document for the national strategy to promote the Belt's development.

[55] Lu S, Liu Q, Xia S and Zhang W 2025 How does industrial transition drive low-carbon transition? evidence from china's resource-based cities *Environ. Dev. Sustain.* **27** 16113–34

[56] Yang D, Liu D, Huang A, Lin J and Xu L 2021 Critical transformation pathways and socio-environmental benefits of energy substitution using a LEAP scenario modeling *Renew. Sustain. Energy Rev.* **135** 110116

[57] Development, N & Reform Commission (NDRC), C 2010 Notice on launching pilot programs for low-carbon provinces and low-carbon cities Chinese. Issued as NDRC Climate [2010] No. 1587. Released on August 10, 2010. The notice initiates pilot work in selected provinces and cities to explore low-carbon development pathways. (available at: www.ndrc.gov.cn/xxgk/zcfb/tz/201008/t20100810_964674.html.)

[58] Development, N & Reform Commission (NDRC), C (NDRC) 2012 Notice on launching the second batch of low-carbon provinces and low-carbon cities pilot programs Chinese. Issued as NDRC Climate [2012] No. 3760. This notice initiates the second round of low-carbon pilot projects in selected provinces and cities, in alignment with China's 12th Five-Year Plan and the national strategy for green and low-carbon development. (available at: https://www.ccchina.org.cn/Detail.aspx?newsId=73289&TId=285)

[59] Jiang B, He Z, Xue W, Yang C, Zhu H, Hua Y and Lu B 2022 China's low-carbon cities pilot promotes sustainable carbon emission reduction: evidence from quasi-natural experiments *Sustainability* **14** 8996

[60] Pan A, Zhang W, Shi X and Dai L 2022 Climate policy and low-carbon innovation: Evidence from low-carbon city pilots in china *Energy Econ.* **112** 106129

[61] Si F, Du E, Zhang N, Wang Y and Han Y 2023 China's urban energy system transition towards carbon neutrality: Challenges and experience of Beijing and Suzhou *Renew. Sustain. Energy Rev.* **183** 113468

[62] Peng L, Mauzerall D L, Zhong Y D and He G 2023 Heterogeneous effects of battery storage deployment strategies on decarbonization of provincial power systems in china *Nat. Commun.* **14** 4858

[63] Peng L, Zhang H and Yan J 2026 Dynamic least-cost pathways for rural china's energy transition away from solid fuels *Commun. Earth Environ.* **7** 660

[64] Fan M, Zhang Z, Wei Y and Sun S 2024 Does innovative city pilot policy improve carbon reduction? quasi-experimental evidence from china *Environ. Res.* **262** 119748

[65] Son H, Kim M and Kim J-K 2022 Sustainable process integration of electrification technologies with industrial energy systems *Energy* **239** 122060

[66] Shen Y, Shi X, Zhao Z, Sun Y and Shan Y 2023 Measuring the low-carbon energy transition in chinese cities *iScience* **26** 105803

[67] Duan H, Mu T and Yu Q 2025 City-level analysis of carbon reduction potential and decarbonization challenges in China *Cities* **158** 105636